A Hierarchical Two-Stage Energy Management for a Home Microgrid Using Model Predictive and Real-Time Controllers

Mahmoud Elkazaz [a,b], Mark Sumner [a], Eldar Naghiyev [a], Seksak Pholboon [a], Richard Davies [a], David Thomas [a]

[a] Power Electronics, Machines and Control Research Group, The University of Nottingham, Nottingham NG72RD, UK
[b] Department of Electrical Power & Machines Engineering, Tanta University, Tanta 31511, Egypt.

ABSTRACT

This paper presents a hierarchical two-layer home energy management system to reduce daily household energy costs and maximize photovoltaic self-consumption. The upper layer comprises a model predictive controller which optimizes household energy usage using a mixed-integer linear programming optimization; the lower layer comprises a rule-based real-time controller, to determine the optimal power settings of the home battery storage system. The optimization process also includes load shifting and battery degradation costs. The upper layer determines the operating schedule for shiftable domestic appliances and the profile for energy storage for the next 24 hours. This profile is then passed to the lower energy management layer, which compensates for the effects of forecast uncertainties and sample time resolution. The effectiveness of the proposed home energy management system is demonstrated by comparing its performance with a single-layer management system. For the same battery size, using the hierarchical two-layer home energy management system can achieve annual household energy payment reduction of 27.8% and photovoltaic self-consumption of 91.1% compared to using a single layer home energy management system. The results show the capability of the hierarchical home energy management system to reduce household utility bills and maximize photovoltaic self-consumption. Experimental studies on a laboratory-based house emulation rig demonstrate the feasibility of the proposed home energy management system.

Keywords:

Hierarchical home energy management system, Model predictive control, Mixed-integer linear programming, Battery energy storage system, Real-time controller.

1. Introduction

Home Energy Management Systems (HEMS) are now being considered as an effective method to reduce home electricity bills and ensure a significant drop in peak energy demand by controlling household

distributed energy resources and shiftable home appliances [1]. The integration of HEMS with Home Battery Storage Systems (HBSS), Demand-Side Management (DSM) techniques and real-time-pricing schemes is receiving much attention in the research literature [2]. There is an increasing trend towards encouraging local consumption of energy generated from renewable energy resources (RES) at the lowest levels of the grid to reduce the export of surplus to the main grid [3]. This includes integrating energy storage systems into homes to use surplus photovoltaic (PV) energy or low cost (off-peak) utility energy at peak-tariff times [4].

Many researchers have focused on optimizing home energy management using approaches such as optimal controllers or real-time decision-making controllers. Using optimal controllers, researchers presented home energy management as an optimization problem with multiple variables and multiple constraints, where the variables are both discrete and continuous [5]. The authors in [6] used Mixed Integer Linear Programming (MILP) optimization to determine the optimal operation of a home with a home battery, a PV system, and an electric vehicle (EV). To study dynamic pricing and peak power limiting based on a DSM strategy, a MILP model of the HEMS was established in [7] with an EV and a HBSS. Although the authors claim a 15 minute sample time for the MILP optimization process, all the results presented have a 1 hour sample time.

A MILP model of a HEMS, as well as an Artificial Neural Network (ANN) for forecasting of residential loads, is described in [8]. The energy management system (EMS) and ANN forecasting model used a sample time of 1 hour for the forecasted home load profiles, which cannot be considered as a real indication of the home's true load profile. [9] developed an optimization strategy to efficiently consider price-based demand response techniques for HEMS; a versatile convex programming framework was constructed for the management of various home appliances. Another energy management scheme which integrates RES, electrical battery storage, and vehicle to grid was proposed in [10]. The authors claim accurate results but run the algorithm only once every day and use a time slot of 1 hour for management which leads to inaccurate results due to uncertainty of the RES and load demand. To tackle the problem of uncertainty with the forecasted energy consumption/generation and update key parameters, researchers have used model predictive control (MPC) to modify and update uncertain parameters and external variabilities for energy management studies [11].

NOMENCLATURE

$E_{actual}(t)$	Actual stored energy in the battery at a time interval t (kWh).	$Prate_{appl}(i)$	Rated electrical power of appliance '*i*' (kW)
E_{MPC}	Stored energy profile for the next 24 hour, obtained from the model predictive control layer (kWh).	$T_{cycle}(i)$	Time needed to complete a full operating cycle for appliance '*i*' (h)
$E_{maximum}$	Mmaximum limit for the energy stored in the battery (kWh).	$б_{startup}(i,t)$	Binary variable to indicate when the appliance has started.
$\boldsymbol{C_{home}}$	Daily household electrical energy costs (£).	$P_{GCP}(t)$	Electrical power at the grid connection point at a time interval t (kW). A positive value means that the home is importing power from the supply utility (grid) while a negative value means exporting power to the supply utility.
$\boldsymbol{C_{home\ buy}}$	Cost of the electrical energy purchased from the main utility per day (£).	$P_{home_{load}}(t)$	Household electrical load demand at a time interval t (kW).
$\boldsymbol{C_{home\ sell}}$	Cost of the exported electrical energy to the main utility per day (£).	$P_{PV\ gen}(t)$	Electrical power generated by the household PV system at a time interval t (kW).
$\boldsymbol{C_{sc}}$	Daily standing charge cost (i.e. £0.24)	$P_{sh\ appl}(i,t)$	Electric power drawn by the controllable (shiftable) home appliance '*i*' at a time interval t
$\Delta\boldsymbol{T}$	Sample time (h)	$P_{HBSS}(t)$	Electric power charged/discharged by the HBSS at a time interval t (kW), where a negative value means that the HBSS is charging, and a positive value means that the HBSS is discharging.
$\boldsymbol{TR_{buy}(t)}$	Electricity purchase tariff at a time interval t (£/kWh).	$E(t)$, $E(t-1)$	Stored energy in the HBSS at a time interval t and t-1 respectively (kWh).

$\boldsymbol{TR_{sell}(t)}$	Selling electricity tariff at a time interval t (£/kWh).	η_d , η_c	Battery discharging and charging efficiencies respectively (%).
$\boldsymbol{\eta_{Conv}}$	Efficiency of the power converter (%).	$B_{capacity}$	Capacity of the battery (kWh).
$\boldsymbol{SOC(t)}$	Battery state of charge at a time interval t (%).	$P_{HBSS}{}^{disch}(t)$	HBSS discharge power at a time interval t (kW)
$\boldsymbol{P_{HBSS\,rat}}$	Maximum HBSS charge/discharge power at time interval t (kW).	$P_{HBSS}{}^{charg}(t)$	HBSS charge power at a time interval t (kW)
$\boldsymbol{SOC_{max}}$	HBSS state of charge maximum limit (%) (i.e. 90%)	$б_{disch}(t)$, $б_{charg}(t)$	Binary variables used to ensure that the HBSS power flows in one direction only at each sample time (i.e. only charging or discharging).
$\boldsymbol{SOC_{min}}$	HBSS state of charge minimum limit (%) (i.e. 20%)	C_{HBSS_d}	The battery degradation cost (£)
$\boldsymbol{CC_{bat}}$	The capital cost of the HBSS (£)	$б_{appl}(i,t)$	binary status of the shiftable appliance '*i'* at time interval t.
$\boldsymbol{\Delta L}$	Lifetime degradation of the battery	$T_{max\ wait}(i)$	Maximum waiting time for appliance *i* to start (h)
$\boldsymbol{N_{cycle}}$	Number of life cycles of the HBSS	$Tstart_{signal}(i)$	Time at which the HEMS receives an ON switch signal for appliance *i* (h)

Most Energy Management Systems (EMS) reported in the literature are based on optimal controllers [12]. Loads and energy resources must be predicted in advance, making the effectiveness of optimal approaches dependent mainly on the accuracy of the prediction models. Computation times can also be significantly longer for these optimal EMS, particularly when using many constraints and shorter sample times. When the behavior of the system cannot be captured by the prediction models or cannot be implemented in real-time, controllers with real-time decision-making capabilities are used. These can be based on instantaneous power measurements rather than prediction profiles as in [13] or on rules ("rule-based" control) as in [14]. For these types of EMS, the aim is usually to reduce energy costs by efficient use of a battery and maximizing the use of renewable energy to satisfy local demand, while maintaining the reliability of the electrical system. They do not require a detailed model of the system and can respond quickly to changes in the system. However, they are not guaranteed to be optimal and this can lead to inefficient energy usage due to lack of oversight. [15] proposed an EMS for optimal battery operation

for electricity distribution grids in the presence of RES. The EMS was used to maximize the utilization of the distributed RES and prevent reverse power flow in the distribution transformer. [16] developed a control strategy for optimal use of a battery storage system in order to integrate the dispatchable intermittent RES. The study suggested a rule-based control scheme as the solution to the optimal control problem defined without violating any battery operating constraints such as state of charge (SOC) limits, discharging/ charging current limits and lifetime. Using a rule-based controller which controls the battery, [16] takes into account only the current situation without considering any future changes in the system and this may lead to impaired system performance.

Most of the EMS introduced in the literature have neglected the economic effects on the system behaviour when there are uncertainties in the forecasts [17], or they operate with long sample times [18], or have assumed no degradation costs for battery operation [19]. The impact of load shifting with a battery system has also not been properly addressed [20].

This paper presents a hierarchical two-layer HEMS which combines the use of an optimization layer and a control layer and highlights the differences between the ideal scheme and real operation with a user-interactive control algorithm. System optimization and real-time control are combined. The hierarchical HEMS minimizes household energy costs, maximizes PV self-consumption and minimizes the system dependence on external forecasting packages whilst also taking into account the battery degradation costs and the opportunity for load shifting. The hierarchical HEMS consists of two layers: (a) The upper layer (Model Predictive Control (MPC) layer) and, (b) The lower layer (Real-Time Controller (RTC) layer). The upper layer comprises an MPC which optimizes household energy usage using a Mixed Integer Linear Programming (MILP) optimization. The lower layer consists of an RTC which controls the Home Battery Storage System (HBSS) while minimizing the energy wastage (local generation exported to the supply utility) that results from forecasting uncertainties and sample time resolution.

The following points summarize the main contribution of this work:

- The hierarchical two-layer HEMS represents an optimization-based real-time interactive algorithm that minimizes the household energy costs and energy wastage, maximizes PV self-consumption while taking into account the battery degradation costs and the use of load shifting. The degradation cost model of the battery was developed to accurately reflect the explicit battery degradation process and its effect on the daily and annual energy costs.
- The upper layer (MPC) focuses on the energy scheduling to ensure the best economic use of electrical energy in the home. The lower layer (RTC) compensates for the effect of forecast uncertainties and the long sample time of the upper layer to guarantee lower household energy costs and minimize energy wastage. It also minimizes the RES power fluctuations and smooths the fluctuations of the electric

power exchange at the point of common coupling with the utility which benefits both the householders and external grid. It updates the upper layer with any disturbances that appear by providing regular feedback.

- The hierarchical HEMS enables the battery to be controlled in real-time, using the RTC, under the supervision of an MPC. Therefore, it responds to any changes in the system (i.e. changing of loads and PV generation) that happen over a short time, which helps in minimizing the daily energy wastage and compensating for RES power fluctuations.
- The two-layer HEMS is considered an improvement over HEMS reported in the literature, as it compensates for the effect of forecast uncertainties, compared to [10], and the effect of sample time resolution compared to [21] while minimizing the computational requirements.

In the context of comparing this paper with other publications that considered hierarchical multi-layer EMSs, this paper actively eliminates the impacts of uncertainty in a timely manner and provides a cost effective real-time corrective action, after the occurrence of uncertainty. This is compared to the approach reported in [22] which used corrective methods based on new optimization calculations in the lower layer. [22] requires time consuming computations, may fail to calculate desired set points in time after the occurrence of an unpredicted incident, and requires a longer computation time for systems with higher numbers of uncertainties. [23] uses very short-term forecasting in the lower control layer, which makes the system highly susceptible to uncertainties in the prediction of household consumption and RES and minimizes the RES self-consumption ratio. The proposed hierarchical two-layer HEMS is more suitable for homes with a large number of controllable devices (i.e. shiftable loads, controllable loads) and RES, compared to [24] which uses an economic load dispatch at the lower control level: this needs more computation time and may fail to obtain the optimal solution for a large number of units and constraints.

Compared with approaches to HEMS such as [25] (which only considers the day-ahead scheduling of home energy resources) and [26] (which ignores the uncertainties associated with the operation of the system), the novelty of the proposed HEMS relies on combining the following points: (a) system coordination of both the day-ahead scheduling and the actual operating stages to appropriately consider the influence of uncertainty in RES and consumption. (b) The use of a HBSS control in both the day-ahead and the actual operation stages. (c) The system links the multiple controllable household appliances with the real-time control of the HBSS to maximize the self-consumption of the RES and compensates for uncertainties. (d) It is computationally efficient by using RTC in the lower control layer, therefore enabling the approach to longer control windows where point prediction is not applicable. (e) It considers demand response flexibility of household appliances – other approaches e.g. [27] do not.

The rest of the paper is arranged as follows: Section II introduces the hierarchical two-layer HEMS. Section III presents the formulation of the MILP-optimization problem and includes the HBSS model, the

battery degradation model and the modelling of the shiftable load. Section IV presents the case study used in this paper. Section V shows the single-layer HEMS including performance analysis and the experimental results. Section VI presents the results obtained using the hierarchical two-layer HEMS. Finally, conclusions are presented from this work.

2. Hierarchical Home Energy Management System

2.1 The Model Predictive Controller layer (upper layer)

The upper layer of the HEMS comprises an MPC, as shown in Fig 1., which optimizes household energy usage. The authors employ a MILP optimization process incorporated with an MPC framework, since the forecast uncertainty can be potentially compensated with a feedback mechanism. The MILP optimization problem is formulated to minimize the daily home household energy costs, maximize the PV self-consumption and minimize energy wastage.

The MPC performs an operation optimization process at each time step for a finite control horizon of the home microgrid to optimize its operation in relation to specified criteria. At each time step (t), a finite horizon optimal control sequence is computed, and an optimal solution is obtained for this period of time. However, only the first step of these control actions is applied. At the next time step (t+1), new measurements of the variables are requested, and with these updates, the optimal control settings are recalculated for the following periods. The main advantage of the MPC is that it optimizes the system for the current sample while keeping account of future changes that will happen.

The upper layer (MPC) focuses on the energy scheduling and ensures the best economic use of electrical energy in the home. Every sample time, the upper layer (1) requests the forecasted household consumption and PV generation profiles for the next 24 hours. It also requests the real-time measurements of the state of charge of the HBSS to update the control model, (2) A MILP optimization process is performed to determine the 24-hour profiles with 15-minute resolution for (a) the stored energy, required for optimal battery operation, i.e. this profile is sent to the lower energy management layer (RTC layer), (b) appliance scheduling. The appliance scheduling profiles are used to control the shiftable appliances, i.e. these profiles are sent directly from the MPC layer to the specific appliances. These steps are repeated every 15 minutes using a rolling horizon approach to update the input variables and obtain new updated settings. These settings will guarantee the best economic use of electrical energy in the home.

2.2 The Real-Time Controller Layer (lower layer)

The lower layer consists of a RTC, which determines the optimal power settings of the HBSS in real-time every one minute using (a) the stored energy profile for the next 24 hours $\mathrm{E}_{\mathrm{MPC}}(t)$ (i.e. obtained from

the upper energy management layer), and (b) a rule-based algorithm. Fig. 2. shows the rule-based operating algorithm for the RTC. The lower layer (RTC) (a) compensates for the effect of forecast uncertainties and the long sample time of the upper layer to guarantee lower household energy costs and less energy wastage, (b) minimizes the RES power fluctuations, (c) smooths the fluctuations of the electric power exchanges at the point of common coupling with the utility, and (d) updates the upper layer with any disturbance that may appear by sending feedback every one minute. The lower layer also sends feedback to update the upper layer with the actual SOC of the HBSS. The upper layer uses this feedback to update the initial SOC of the battery, which is essential to perform the subsequent optimization process (new energy scheduling).

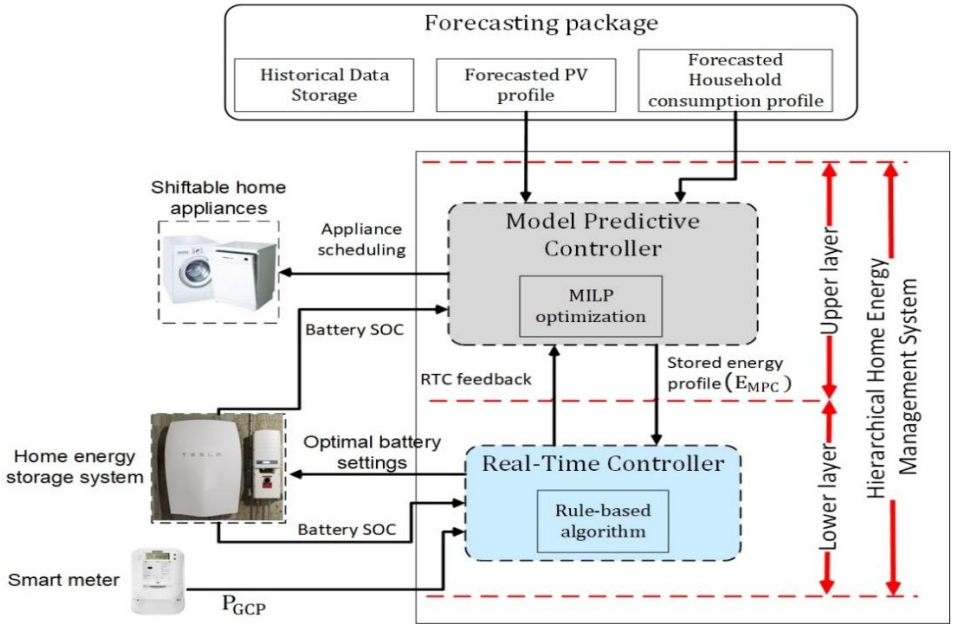

Fig. 1. Hierarchical scheme of the two-layer home energy management system including both the upper and the lower management layers.

3. System modelling and formulation of the MILP-optimization problem

The minimization of the daily household energy costs is formulated as a MILP optimization problem. The general mathematical formulation of the MILP problem is presented in [28]. The daily household energy cost, "C_{home}", which needs to be minimized, can be formulated in terms of payments and incomes. The payments include the cost of electricity purchased from the utility, the battery degradation cost and the standing charge, see equations (1) and (2). The incomes are the revenue from the energy exported to the utility, i.e. the excess electricity from the PV generation after charging the HBSS and satisfying the home demands, see equations (1) and (3).

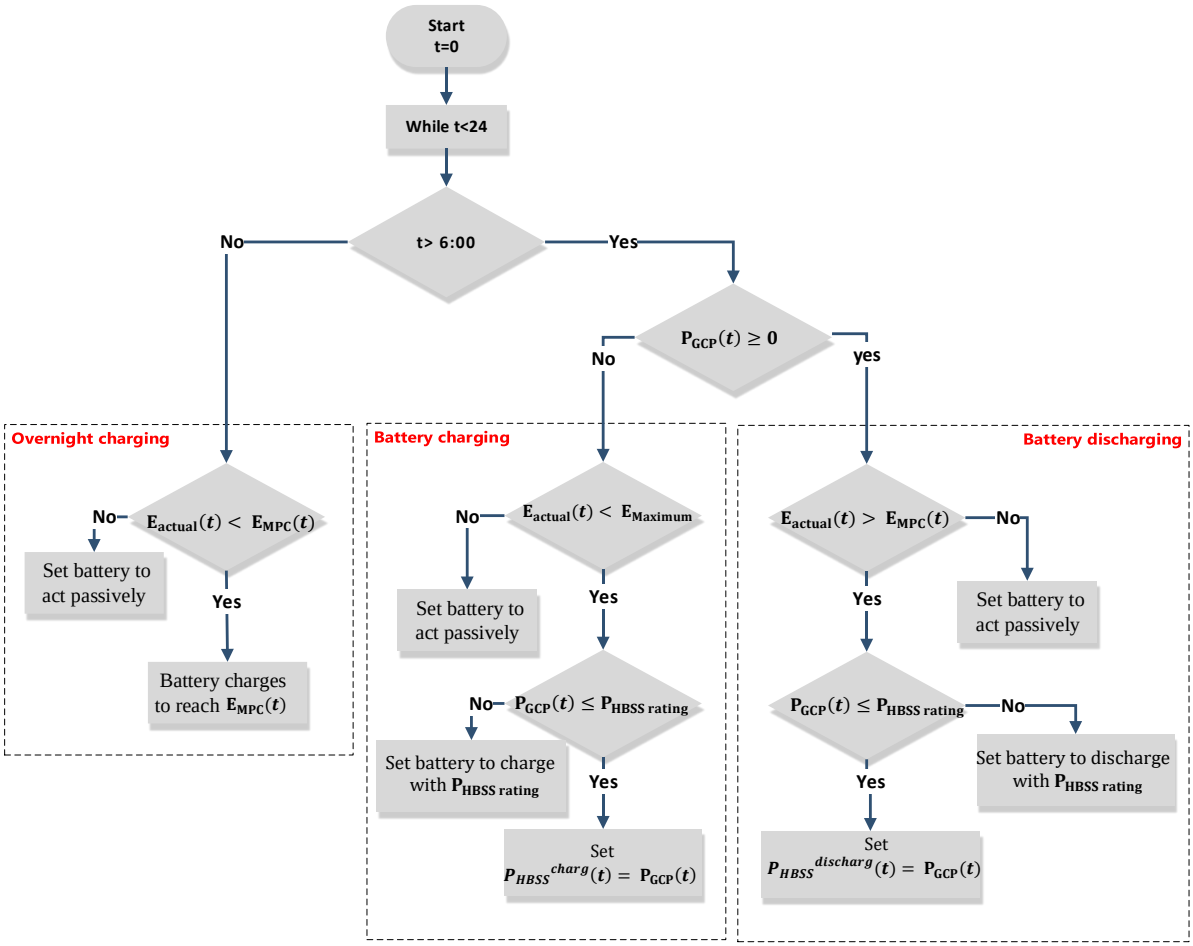

Fig. 2. Flowchart of the rule-based control algorithm for the real-time controller.

$$C_{home} = C_{home\_buy} + C_{home\_sell} + C_{HBSS_d} + C_{sc} \quad (1)$$

$$C_{home_{buy}} = \sum_{to}^{T} \Delta T \times TR_{buy}(t) \times P_{GCP}(t) \quad , P_{GCP}(t) > 0 \quad (2)$$

$$C_{home\_sell} = \sum_{to}^{T} \Delta T \times TR_{sell}(t) \times P_{GCP}(t) \quad , P_{GCP}(t) < 0 \quad (3)$$

where C_{home} is the daily cost of household electrical energy (£). C_{home_buy} is the cost of the electrical energy purchased from the utility per day (£). C_{home_sell} is the cost of the exported electrical energy to the utility per day (£). C_{HBSS_d} is the daily battery degradation cost (£). C_{sc} is the daily standing charge cost (i.e. 24 pence per day). ΔT is the sample time (hours). $P_{GCP}(t)$ is the electrical power measured at the grid connection point (kW) at a time interval t; a positive value means that the home is importing power from the utility while a negative value means exporting power to the utility. $TR_{buy}(t)$ is the electricity purchase tariff at a time interval t (£/kWh). $TR_{sell}(t)$ is the electricity sale tariff at a time interval t (£/kWh).

The total active power balance equation of the home is represented by (4).

$$\mathrm{P}_{GCP}(\mathrm{t}) + \mathrm{P}_{\mathrm{HBSS}}(t) = \ \mathrm{P}_{home_{load}}(t) + \mathrm{P}_{\mathrm{sh\ appl}}(\mathrm{i},\mathrm{t}) - \mathrm{P}_{\mathrm{PV_{gen}}}(t) \tag{4}$$

where $\mathrm{P}_{\mathrm{HBSS}}(t)$ is electric power discharged/charged by the HBSS at a time interval t (kW), where a positive value means that the HBSS is discharging, and a negative value means that the HBSS is charging.$P_{home\_load}(t)$ is the household electrical load demand at a time interval t (kW). $P_{sh\ appl}(i,t)$ is the electric power drawn by the controllable (shiftable) home appliance 'i' at a time interval t (kW). $P_{PV\_gen}(t)$ is the electrical power generated by the household PV system at a time interval t (kW).

3.1. Modelling of the Home Battery Storage System

The model of the HBSS is represented as follows.

The stored energy in the battery, every sample time, can be formulated as (5).

$$E(t) = \ E(t-1) \ - \frac{\Delta\mathrm{T} \times {P_{HBSS}}^{disch}(t)}{\eta_{\mathrm{d}}} - \ \Delta\mathrm{T} \times \eta_{\mathrm{c}} \times {P_{HBSS}}^{charg}(t) \tag{5}$$

where $E(t)$ and $E(t-1)$ are the stored energy (kWh) in the HBSS at a time interval t and t-1 respectively. ${P_{HBSS}}^{disch}(t)$ and ${P_{HBSS}}^{charg}(t)$ are respectively the HBSS discharge and charge powers at a time interval t (kW). ${P_{HBSS}}^{disch}(t)$ is always a positive value while ${P_{HBSS}}^{charg}(t)$ is always a negative value. η_{d} , η_{c} are the battery discharging and charging efficiencies respectively (%). These are assumed to be constant values, neglecting the variation of the efficiency for different values of charging or discharging power.

The status of the stored energy of a battery every sample time is defined as state of charge (SOC), see (6):

$$\mathrm{SOC}(\mathrm{t}) = \frac{\mathrm{E}(\mathrm{t})}{\mathrm{B}_{\mathrm{capacity}}} \times 100 \tag{6}$$

where $\mathrm{B}_{\mathrm{Capacity}}$ is the capacity of the battery (kWh).

Minimum and maximum SOC level constraints (7), are used to avoid overcharging or deep discharging the HBSS, as this can significantly reduce the battery lifetime [29]. This constraint is recommended by the IEEE [30] and is critical to the HBSS operation. The SOC limits of the lithium-ion battery, considered in this research, are restricted to a range between 20 and 90 % of the nominal battery capacity.

$$\mathrm{SOC}_{\mathrm{min}} \leq \mathrm{SOC}(\mathrm{t}) \leq \ SOC_{\mathrm{max}} \tag{7}$$

where SOC_{max} and SOC_{min} are the maximum and minimum allowable SOC limit (%).

The model of the battery power converter is represented by (8). The battery power converter acts as an interface between the battery and the HEMS and is used to control the battery.

$$\mathrm{P_{HBSS}(t)} = {P_{HBSS}}^{disch}(t) \times \eta_{\mathrm{Conv}} + \frac{{P_{HBSS}}^{charg}(t)}{\eta_{\mathrm{Conv}}} \qquad (8)$$

where $P_{HBSS}(t)$ is the charged/discharged electrical power from the HBSS at a time interval t (kW), where a negative value means the HBSS is charging, while a positive value means the HBSS is discharging. η_{Conv} is the efficiency of the power converter (%). The efficiency of the power converter is assumed constant in this research.

The HBSS power output constraint (9), reflects the operating limits of the HBSS and defines the maximum power that can be discharged/charged by the HBSS.

$$-\mathrm{P_{HBSS\ rating}} \leq \mathrm{P_{HBSS}(t)} \leq \mathrm{P_{HBSS\ rating}} \qquad (9)$$

where $\mathrm{P_{HBSS\ rating}}$ is the rated (maximum allowable) HBSS charge/discharge power (kW) (i.e. rated converter power).

Two binary variables $б_{disch}(t)$ and $б_{charg}(t)$are introduced to create a link restriction to ensure the battery is not charged and discharged at the same time, i.e. battery power flows in one direction at any given time, see (10-12):

$$б_{disch}(t) + б_{charg}(t) \leq 1 \qquad (10)$$

$$б_{disch}(t) = \begin{cases} 1 & , \mathrm{P_{HBSS}(t)} > 0 \\ 0 & , \mathrm{P_{HBSS}(t)} \leq 0 \end{cases} \qquad (11)$$

$$б_{charg}(t) = \begin{cases} 1 & , \mathrm{P_{HBSS}(t)} < 0 \\ 0 & , \mathrm{P_{HBSS}(t)} \geq 0 \end{cases} \qquad (12)$$

where $б_{disch}(t)$ equals 1 if the battery is discharging and equals 0 otherwise. $б_{charg}(t)$ equals 1 if the battery is charging and 0 otherwise.

Constraints (13, 14) are used to create a link between the battery power and the binary variables $б_{\mathrm{disch}}(\mathrm{t})$ and $б_{\mathrm{charg}}(\mathrm{t})$.

$${P_{HBSS}}^{disch}(t) \leq б_{disch}(t) \times \mathrm{P_{HBSS\ rating}} \qquad (13)$$

$${P_{HBSS}}^{charg}(t) \geq б_{charg}(t) \times -\mathrm{P_{HBSS\ rating}} \qquad (14)$$

The HBSS model feeds into the power calculations of the MILP optimization problem, i.e. $\mathrm{P_{HBSS}}(t)$ in eq. (4), and the constraints (7, 9-14) are considered as MILP optimization constraints.

3.2.Battery degradation model

In order to simultaneously optimize energy cost and battery lifetime, estimated equivalent costs of battery degradation are defined in terms of battery lifetime reduction. [31] divided the battery degradation cost into three parts: SOC related degradation, temperature related degradation, and the depth of discharge (DOD) related degradation. The temperature related degradation is caused by the fluctuations in charging power or discharging power. It is negligible for the HBSS since their discharging/charging current and voltage are usually stable. The DOD related degradation is considered the capacity fade resulting from the daily minimum SOC level achieved during battery operation [32]. The manufacturers of the batteries quantify the life of the battery (i.e. the number of cycles until the end of life) as a function of the DOD. The lifetime throughput can be calculated using the information available in the battery specification sheet [33]. For home battery storage, the HEMS keeps the DOD (i.e. minimum SOC level) of the battery within certain limits to maximize the lifetime of the battery. The SOC related degradation is considered as a function of the daily number of the charging and discharging cycles.

In this research, the daily cost of battery degradation (C_{HBSS_d}) due to DOD and the number of charging and discharging cycles is defined as (15) [34] .

$$C_{HBSS_d} = \mathrm{CC_{bat}} \times \frac{\Delta \mathrm{L}}{N_{cycle}} \tag{15}$$

where $\mathrm{C_{HBSS_d}}$ is the battery degradation cost (£). $\mathrm{CC_{bat}}$ is the capital cost of the battery (£). $\Delta \mathrm{L}$ is the lifetime degradation. $\mathrm{N_{cycle}}$ is the number of life cycles undergone by the battery.

(15) has been formulated into a linear equation (16) by using (5) and (8).

$$C_{HBSS_d} = \sum_{to}^{\mathrm{T}} \frac{\mathrm{CC_{bat}} \times \eta_{\mathrm{Conv}} \times \eta_{\mathrm{c}} \times \Delta \mathrm{T} \times {P_{HBSS}}^{charg}(t)}{2 \times \mathrm{N_{cycle}}} + \frac{\mathrm{CC_{bat}} \times \Delta \mathrm{T} \times {P_{HBSS}}^{disch}(t)}{\eta_{\mathrm{Conv}} \times \eta_{\mathrm{d}} \times 2 \times \mathrm{N_{cycle}}} \tag{16}$$

The battery degradation model is used in the cost function equation (1) to account for the battery degradation costs into the optimization problem.

3.3.Shiftable appliances modelling

In this section, the modelling of the shiftable home appliances is presented. Operation of some home appliances, such as washing machines, dishwashers, dryers, etc. can be shifted in time to avoid operating them at peak tariff periods. The upper layer of the HEMS determines the best scheduling of the home appliances to achieve lower energy costs for householders. It is assumed that the user sends a switch ON signal to the HEMS to enable the start of an appliance ‘i’. The HEMS receives the ON switch signal, for appliance ‘i’, and schedule for its operation as soon as possible. The HEMS could shift the appliance from

operating at the peak-tariff period to operate at an off-peak tariff period to minimize the household energy costs, or to operate when there is excess PV generation to maximize PV-self consumption. The time which passes between the receiving of ON switch signal and actual operation of the appliance is called the waiting time. The maximum allowable waiting time can be adjusted by householders based on their requirements, i.e. zero waiting time means the immediate start of the device when a switch ON signal is received by the HEMS. If no choice is made it is assumed to be 4 hours to keep a high comfort level for householders. Equation (17) defines the waiting time constraints for each appliance 'i'.

$$\Delta T \times \sum_{Tstart_{signal}(i)}^{24} logic\ NOt(б_{appl}(i,t)) \leq \mathrm{T_{max\ wait}}(i) \quad (17)$$

where $\mathrm{T_{max\ wait}}$(i) is the maximum waiting time of appliance 'i' (h) (i.e. defined by the users). $Tstart_{signal}(i)$ is the time at which the HEMS receives an ON switch signal for appliance 'i' (h). ΔT is the sample time (hour).

$б_{appl}(i,t)$ is a binary variable represents the operation status of a shiftable appliance 'i' at time interval 't', see (18).

$$б_{appl}(i,t) = \begin{cases} 1 & ,if\ ON \\ 0 & ,if\ \mathrm{OFF} \end{cases} \quad (18)$$

A new binary variable $б_{startup}(i,t)$ is introduced to indicate the starting up of an appliance 'i' (i.e. $б_{startup}(i,t)$ equals 1 when the status of an appliance 'i' has changed from OFF to ON and equal 0 otherwise), see (19).

$$б_{appl}(i,t+1) - б_{appl}(i,t) - б_{startup}(i,t) \leq 0 \quad (19)$$

Constraint (20) is used to keep the appliance 'i' in continuous operation for the complete operation cycle without being switched OFF.

$$\Delta T \times \sum_{Tstart_{signal}(i)}^{24} б_{appl}(i,t) = \mathrm{T_{cycle}}(i) \quad (20)$$

where $\mathrm{T_{cycle}}(i)$ is the time needed (h), for an appliance 'i', to complete a full operating cycle.

To avoid starting any appliance without a request from the user, and also to ensure the appliance is switched OFF after completing its operating cycle, the appliance status $б_{appl}(i,t)$ is set to 0 before the HEMS receives the start signal for appliance 'i' and after finishing the operating cycle.

$$\mathbf{б_{appl}(i,t) = 0 \qquad Tstart_{signal}(i) > t\ ,\ \ t > Tend} \quad (\mathbf{21})$$

Finally, the power drawn by shiftable home appliance 'i' at any time period can be represented by (22).

$$\mathrm{P_{sh\ appl}(i,t)} = \mathrm{Prate_{appl}(i)} \times б_{appl}(i,t) \qquad (22)$$

where $\mathrm{Prate_{appl}(i)}$ is the rated electrical power of appliance '*i*' (kW).

The shiftable appliances models feed into the power calculations of the MILP optimization problem, i.e. $\mathrm{P_{sh\ appl}(i,t)}$in eq. (4), and the constraints (17-21) are considered as MILP optimization constraints.

4. Case study

The case study used in this paper is for a UK based house which includes, besides the common home appliances, a rooftop PV system and a HBSS. Also, the house is connected to the grid to import any further required energy and export any excess PV energy (i.e. after satisfying the household load demands and charging the HBSS). The household load profiles used in this paper are based on actual measurements for a load demand of a house located in the UK [35]. This data is for one year and of one minute resolution. The annual electricity consumption of the house studied was 4104 kWh, which is close to the UK average of 4200 kWh for medium type users [36]. This data was combined with a real PV generation profile of a 3.8 kW rooftop PV located in the UK [37]. The data is for 12 months with a resolution of one minute. The PV generation profiles were scaled down to be equivalent to the PV generation of 1.4 kW peak system, which was assumed to be suitable for the home under study.

The electricity tariff schemes used in this research are (a) Time of Use (TOU) tariff scheme for the purchased electric energy from the utility, and (b) fixed feed-in tariff scheme for exporting electricity to the utility. The TOU purchasing tariff values, shown in Table 1, are obtained from the Green Energy Company, UK [38]. A standing charge of 24 pence per day is also considered as a part of the TOU tariff scheme to pay for Distribution Network Operator (DNO) costs. A fixed feed-in tariff value of 3.79 pence/kWh has been used in this research. This value is obtained from the Ofgem website for feed-in tariffs in the UK [39]. Similar tariffs are available in other countries [40].

Table 1.

Unit cost values for TOU purchasing tariff scheme at each time period.

Time (h)	Unit cost (pence/kwh)
23:00 to 06:00	4.99
06:00 to 16:00	11.99
16:00 to 19:00	24.99
19:00 to 23:00	11.99

The size of the battery has been selected using the model presented in [41] for calculating the optimal size of an energy storage system. The size of the battery is selected to minimize the annual household energy costs (investment and operational costs) and maximize the PV self-consumption. The investment cost is the initial cost of the HBSS (the battery and the power converter), while the operational costs are the daily household energy costs shown in equations (1-3). The following values have been used for the battery sizing model: (a) battery energy rating investment cost of £135/kWh [42], and (b) power rating investment cost of £130/kW [43]. The installation cost of the HBSS is assumed to be £500. The nearest available commercial size of the battery and the power converter has been selected using the results obtained from this model. Table 2 shows the parameters of the home battery storage system [44], and the battery power converter [45] used in this research.

Table 2.

Parameters of the home battery storage system and the battery power convereter used in this study.

Battery capacity ($\mathrm{B_{capacity}}$)	6.4 kWh	Converter rated power ($P_{HBSS\ rating}$)	±2.5 kW
Battery efficiency (η_{d}, η_{c})	95.3 %	Converter efficiency (η_{Conv})	96.7 %
$\mathrm{SOC_{min}}$	20 %	SOC_{max}	90 %
Capital cost of the battery ($\mathrm{CC_{bat}}$)	£ 1230	Number of life cycles of the battery ($\mathrm{N_{cycle}}$)	5000

Next day load demand and PV generation forecasting are essential for the operation of the MPC layer. The MPC layer needs the household consumption profile and PV generation profile for the next 24 hours to perform the optimization process. There are several forecasting methods that could be used to forecast the household consumption and the PV generation for the next day [46].

In this research, the forecasted household consumption profile for the next day is assumed to be the same as the previous week, same day household consumption profile (L-PWSD); while the forecasted PV generation profile for the next day is assumed to be the same as the previous day PV generation profile (PV-PD). Using the historical data for household consumption and PV generation minimizes the dependence on external communication technologies (i.e. no need for complex forecasting packages that require additional meteorological data), which makes this control hierarchy a reasonable solution for remote areas which suffer from a poor communication network.

To assess the performance of the hierarchical HEMS, three performance indicators have been used:

- **Household energy costs**: The actual household energy costs are calculated by solving equations (1).
- **PV self-consumption ratio**: The PV self-consumption ratio is used to measure the amount of PV energy consumed in the home by direct consumption or by storing in the HBSS to be used later. This ratio is calculated by dividing the generated PV energy consumed inside the home by the total generated PV energy.
- **Energy wastage ratio:** Energy wastage ratio is calculated by dividing the total energy exported to the grid by the total PV energy generated. The wastage energy is the unwanted feed-in energy to the utility resulting from (a) inaccurate power settings of the HBSS due to forecasting errors or sample time accuracy, and/or (b) poor estimation of the required overnight charging level of the battery which results from errors in forecasting the next day's energy profile. This may result in the battery incorrectly being fully charged such that excess PV energy cannot be stored. When the energy wastage ratio equals 0%, no lost energy will be observed. As this value increases, more energy wastage will be observed, which therefore leads to more household energy costs and poorer system performance. The wastage energy should be saved in the battery to be used at the correct time instead of being fed into the utility for no or low reward.

5. The performance of the single-layer HEMS

First, the performance of the HEMS was tested using only the single MPC layer. Single-layer HEMS is the most popular approach to battery control in the literature. This experiment is implemented to measure the performance of the single-layer HEMS (i.e. using only the MPC layer) in a real environment using a real HBSS.

5.1. Laboratory-Based Smart Home Rig Architecture

The single-layer HEMS was tested experimentally in a real-time environment for one day at the University of Nottingham's FlexElec Laboratory, using the "Smart Home Rig" (SHR) shown in Fig. 3. and Fig. 4

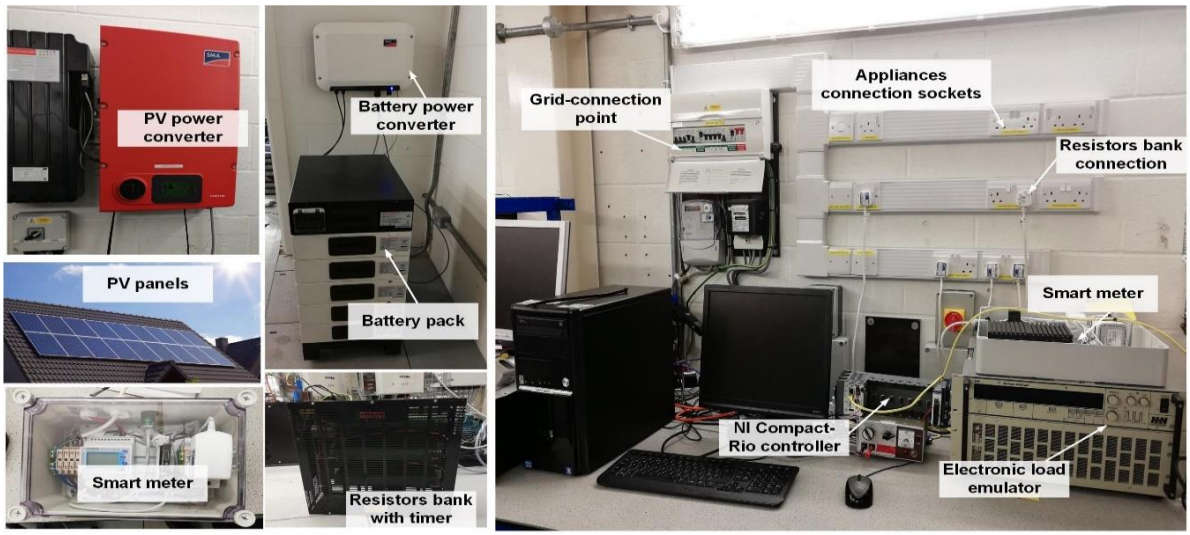

Fig. 3. Architecture of the smart home rig, used in the experiment, at the FlexElec Laboratory, University of Nottingham.

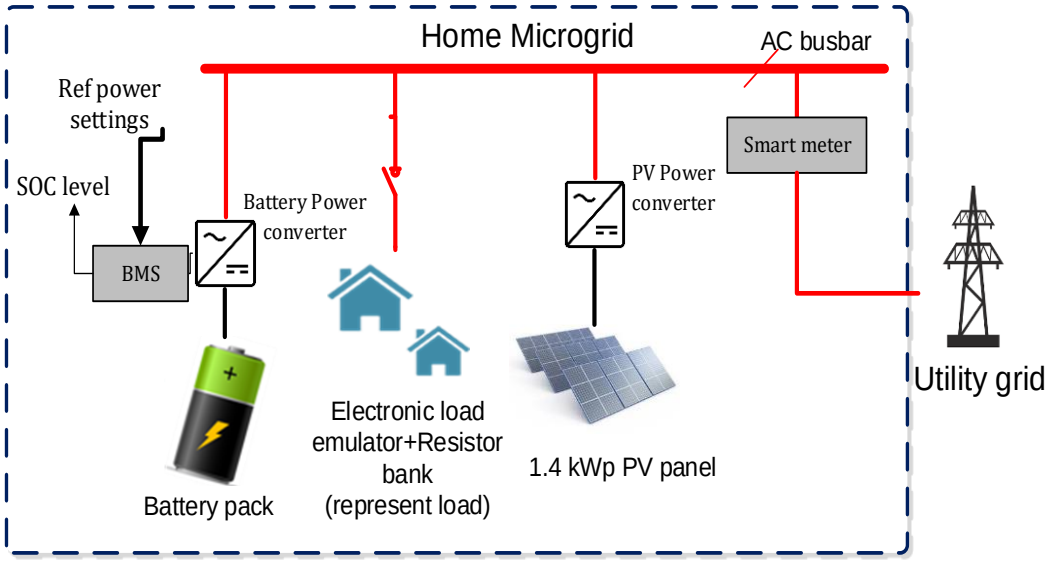

Fig. 4. Connection diagram of the smart home rig at the FlexElec Laboratory, University of Nottingham.

This SHR includes:

- HBSS: consists of a 6.4 kWh BYD lithium-ion battery pack [44], and a 2.5 kW SMA bidirectional power converter [45].
- 1.4 kW peak PV panels connected to a 3.68 kW SMA power converter and connected to the SHR switchboard [47].
- 5.6 kW ZSAC electronic AC load emulator [48], which received the digital daily load demand profile from LabVIEW software, and converted it to actual current absorbed from one of the appliance connection sockets in the SHR. A NI compact Rio controller [49] and LabVIEW software are used to move the digital load profiles from the database to the electronic AC load emulator as a control signal.

- A 1.3 kW resistive load with timer circuit, has been used to represent the washing machine operation. This load acts as a shiftable home appliance.
- A 3 phase smart meter and is used to measure the PV generation power, load demand, and the power at the grid connection point [50].
- A Raspberry Pi used the Modbus protocol to transmit the measured data from the smart meter to the HEMS, and to transmit the measured SOC of the battery to the HEMS regularly. Also, the Raspberry Pi is used to transmit the optimal battery power settings, obtained from the HEMS, to the battery's power converter.
- A PC: Core i3-7100 CPU, 3.91 GHz was used to run a MATLAB software, which in turn ran the HEMS and performed the MILP optimization process.

The software development packages used in this experiment are: (a) MATLAB - used to run the HEMS including performing the MILP optimization process, and (b) LABVIEW - used as a graphical user interface GUI tool to control the electronic AC load emulator.

5.2. Experimental Procedure

The MPC single-layer HEMS was implemented experimentally in real-time such that at each sample time (i.e. two minutes in this experiment): (1) The forecasted household consumption profile, as well as the forecasted PV generation profile for the next 24 hours is obtained from the historical data. (2) The values of the actual SOC level of the HBSS are measured from the battery power converter, and sent to the HEMS using the Raspberry Pi, (3) the MILP optimization process is performed using a MATLAB script. The computational time of the MILP-optimization process, using a two minute sample time, is found to be 104 s. (4) The appliance scheduling profiles obtained, for the next 24 hours, (i.e. ON/OFF status of the shiftable appliances) are sent to each appliance. (5) The HBSS optimal power setting obtained for the next sample time only (t+1), obtained from the MILP optimization process, is sent to the battery power converter using the Raspberry Pi. Using the single-layer HEMS, the HEMS controls the HBSS directly, without using the lower RTC layer, by sending the optimal battery power settings, obtained from the MILP-based optimization process, directly to the battery power converter. (6) The previous steps are repeated every sampling time to update the appliance scheduling and the HBSS optimal power setting.

Using a short sample time for MPC operation enables the single-layer HEMS to respond to any changes in the system (i.e. changing of loads, PV generation, and battery SOC level). This is achieved by scanning the input data and updating battery settings, using a two minute sample time, which achieves better results. Using a longer sampling time will lead to more daily energy costs and more energy wastage. Selecting a proper sample time will be discussed further in section 5.4.

5.3. Results

Fig. 5. shows the operation of the house rig, using the single-layer HEMS, for one day. Fig. 5.a and Fig. 5.b show that the HEMS feeds the household demands at the peak-time hours (from 16:00 to 19:00) using the HBSS instead of importing energy from the utility during the peak tariff period (i.e. when the tariff value is 24.99 pence/kWh). The unwanted imported and/or exported power spikes that are observed in Fig. 5.b (+ve and -ve values of the black profiles start from 07:00) result due to inaccurate forecasting for the load demand and/or PV generation, time delay between the spike occurring and the HBSS reacting, and the battery is limited to 2.5 kW, so cannot cover spikes greater than that. These spikes are the main reason for energy wastage. The daily energy wastage ratio, due to these spikes, is calculated to be 26.98%. This value is not a good value since one quarter of the generated PV energy is exported to the utility with low reward. This energy should instead be stored in the HBSS to be used at the correct time.

It is observed from Fig. 5.d that the HEMS charges the HBSS during the night up to 66% and not up to its maximum limit (i.e. 90%) because it is the optimal overnight charging level. The optimal overnight charging is adjusted to enable the battery to be topped-up by the forecasted surplus PV generation during the following day, and at the same time, feed the forecasted load demand during the morning period (i.e. aim not to purchase energy from the main utility from 6:00 to 10:00). The daily household energy cost for this day, using the single-layer HEMS, is £0.837, i.e. this cost comprises the daily cost of energy imported/exported from the utility, the daily battery degradation cost and the daily standing charge (1).

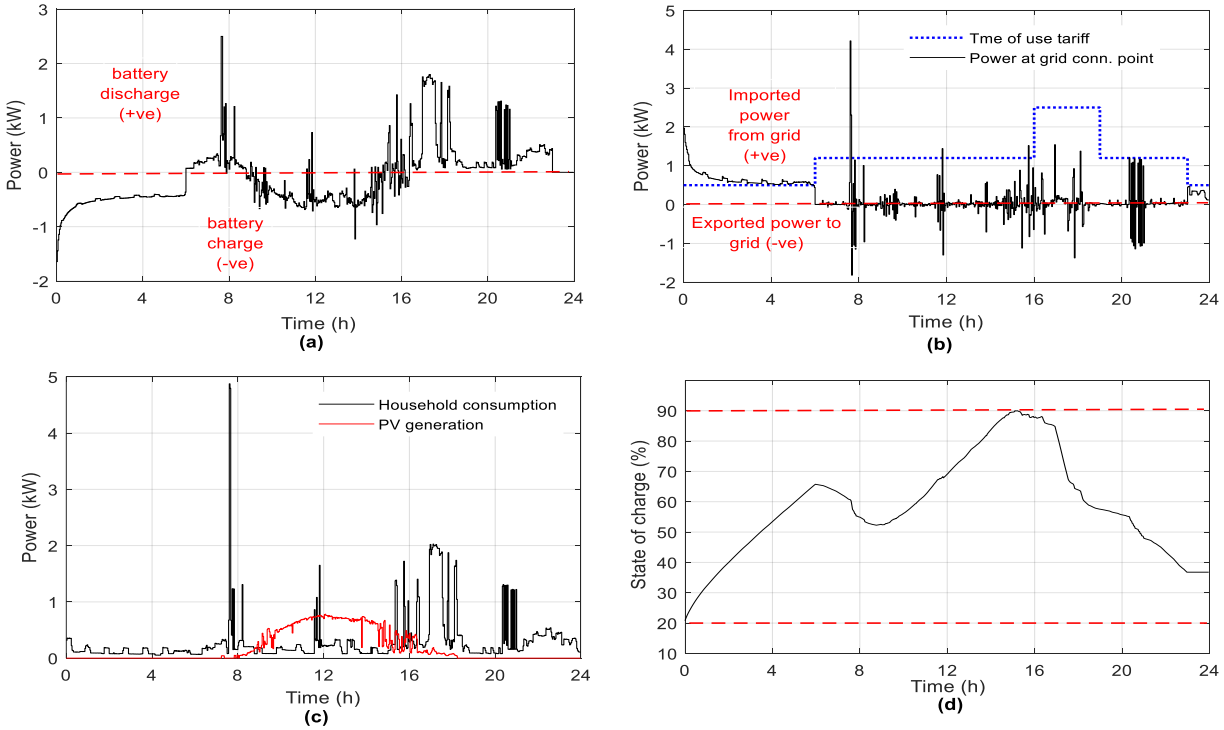

Fig. 5. Experimental house rig results using the single-layer HEMS for one day, (a) the optimal power settings delivered to the HBSS (a positive value means that the HBSS is discharging, while a negative value means that the HBSS is charging), (b) the actual power measured at the grid connection point (a positive value means the house is importing power from the utility, and a negative value means exporting), and the corresponding TOU tariff, (c) the actual household demand and PV generation for the current day, (d) the daily actual state of charge of the HBSS.

The last state point of each horizon in the MPC (i.e. the last point of the SOC of the HBSS) is kept free (i.e. no constraint is set on the state of charge of the battery at the end of the day) to give more flexibility to the MPC to take actions. For example, if there were to be a constraint on the last point of the SOC of the HBSS, on some days the HEMS would be forced to export energy to the utility (at no or low revenue) to keep the SOC of the battery at the end of the day within the set limit. Also, if the actual PV generation was more than the predicted PV generation, the MPC would not store the excess PV energy in the HBSS and instead would export it to the utility (at no or low revenue) to keep the SOC of the battery at the end of the day as constrained. This actually decreases the PV self-consumption ratio and does not ensure the best economic use of electrical energy in the home.

For the shiftable loads (i.e. washing machine in this experiment), it is assumed that the user requested to operate the washing machine at 16:30. The single-layer HEMS shifted the washing machine to operate at 20:30 (mid-peak tariff period) instead of 16:30 (peak tariff period) to reduce the cost of the energy imported from the utility. This is clear from Fig. 6. The single-layer HEMS has not shifted the washing machine to operate at 23:00 (i.e. off-peak tariff period), because the maximum waiting time for each appliance is four hours.

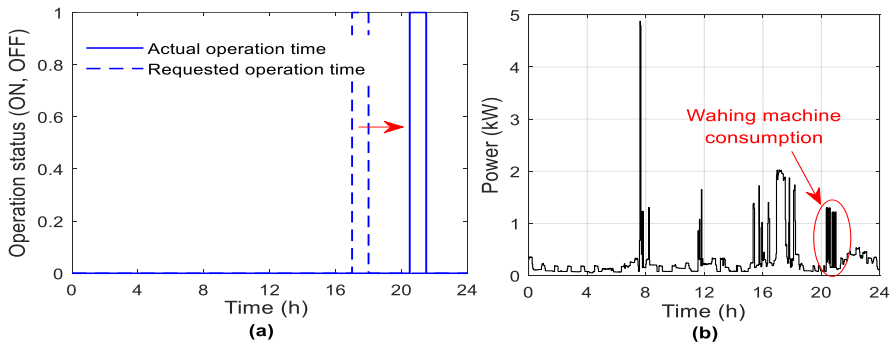

Fig. 6. Daily operating schedule of the washing machine, (a) the requested and the actual operating time of the shiftable washing machine, (b) the actual household power consumption after the operation of the washing machine at 20:30.

5.4. The effect of sample time

Selecting an appropriate sample time is important for the operation of the MPC layer. For example, selecting a 60 minute sample time means that the HBSS optimal power settings obtained from the MILP optimization process will remain constant for 60 minutes. Consequently, any change in load demand and/or PV generation during this 60 minute period will be compensated from the utility grid based on the balance equation of the total active power in the home (4), which may affect the overall energy costs. On the other hand, when selecting a two minutes sample time for the MPC layer operation, the MPC will be able to respond to small changes in load demand and PV generation by updating the HBSS power settings every two minutes in a way that works for minimizing the overall energy costs and minimize energy wastage.

Fig. 7. shows the effect of using a 60 minute sample time versus a 2 minute sample time for MPC operation. The actual load demand and PV generation has been used for prediction in this particular test to study the effect of sampling time only without the effect of forecasting errors. It is clear from Fig. 7.a that when using a 60 minute sample time for MPC operation, the HBSS power settings (red settings) obtained remain fixed for 60 minutes. Consequently, the changes in load demand and PV generation are compensated from the utility as shown in Fig. 7.b (red line). Using a 60 minute sample time leads to purchasing energy from the utility at peak-tariff period (i.e. from 16:45 to 17:30 and from 18:00 to 18:15) at a high cost. Also, excess PV energy is exported to the grid during the period 17:30 to 18:00. This unwanted exported energy could be stored in the HBSS to be used later instead of selling it at a low price.

When using a two minute sample time, Fig. 6.a shows that the MPC layer updates the HBSS power settings (blue line) every two minutes to respond to load and PV generation changes (i.e. Fig. 6.c) to avoid buying or selling energy from/to the utility at wrong periods as shown in Fig. 6.b (blue line).

Table 3 shows the effect of using different sample times, for MPC operation, on the daily household energy costs and the daily energy wastage ratio. The forecasted demand and PV generation profiles used in this table are 100% accurate (i.e. zero forecasting error) to clearly study the effect of sample time only.

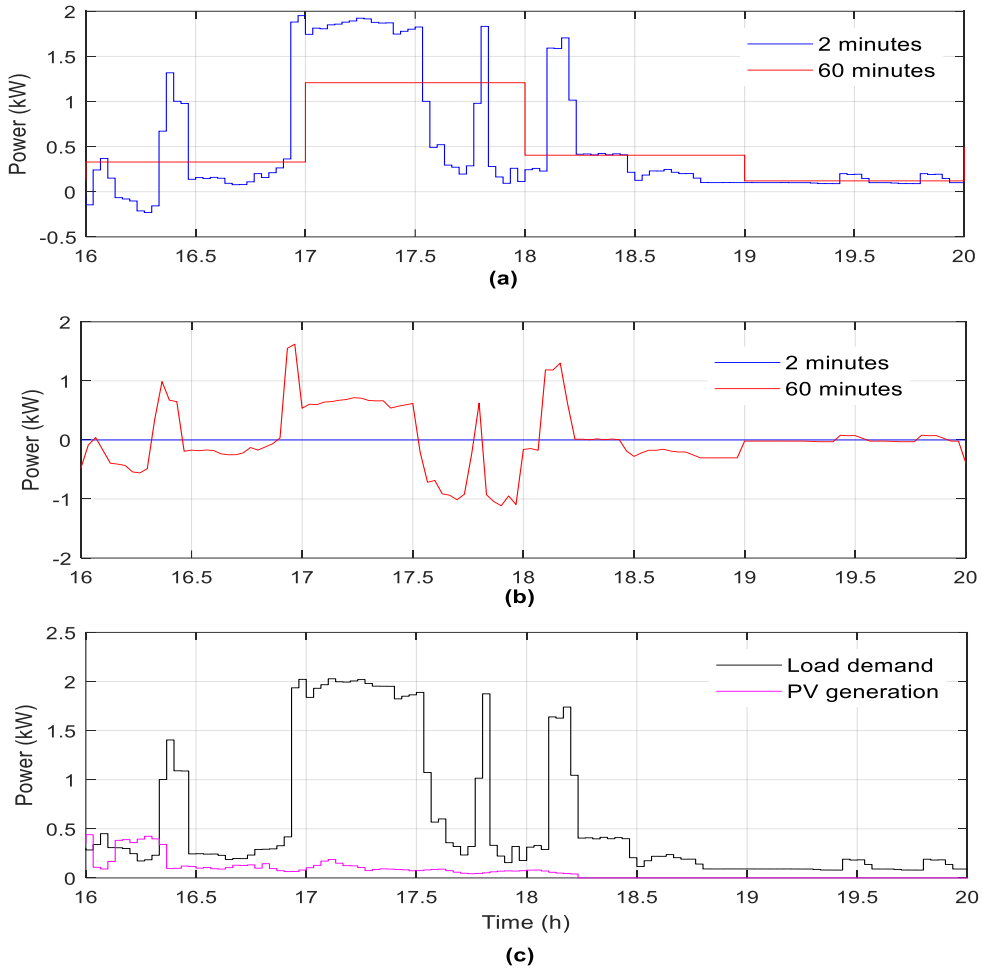

Fig. 7. MPC operation for a sample time of 2 minutes and 60 minutes, (a) The HBSS optimal power settings in case of using a 60 minute (red settings) and in case of using a 2 minute (blue settings), (b) the resultant power at the grid–connection point in case of using a 60 minutes sample time (red settings) and in case of using a 2 minute (blue settings), (c) load demand and PV generation profile of a 2 minute sample time.

Table 3.

Daily household energy costs, daily energy wastage ratio and MILP computation time under different sample times

Sample time resolution (minutes)	**60**	**30**	**12**	**4**	**2**
Household energy costs (£)	0.815	0.751	0.739	0.639	0.578
Energy wastage ratio (%)	44.68	35.9	30.43	12.85	0.5
Computation time of the MILP optimization (s)	5.16	6.31	7.53	16.3	104

It is obvious from table 3 that if a shorter sample time is used, lower household energy costs and a lower energy wastage ratio are achieved. However, more computation time is needed for the MPC optimization process. It can be seen from Table 3 that the computation time would increase exponentially as a shorter sample time is used. This is a drawback of the optimization method, not a drawback of the single-layer HEMS. As the sample time resolution increases (i.e. shorter sample time), the number of sample points in the optimization process increases, which needs a more powerful computing platform and larger memory, and of course more computational time as the number of optimal points increases. For example, if the sample time is 15 minutes, the number of sample points in the optimization process is 96 (for a 24 hour control horizon) multiplied by the number of variables, e.g. HBSS charging/discharging profile, load profile, PV profile, shiftable appliance's control profile, etc. However, if the sample time is two minutes, the number of points for a 24 hour optimization process is 720, which is then multiplied by the number of variables. Selecting another optimization method such as a Genetic Algorithm or Particle Swarm Optimization may affect the computation results.

Using short sample times for MPC operation may conflict at some points with the computational time of the optimization process. For example, if a one minute sample time is used, and a rolling step of one minute is assumed for MPC operation, the MPC will take 5.62 minutes to perform the optimization process only (i.e. more computation time than the rolling step assumed), which makes it unfeasible to use this sample time. Also, the computation time of the optimization process may be longer if a more complicated system with more constraints and variables is used. Also, using a short sample time (e.g. two minutes) may not be suitable for transient situations, since a very short sample time is needed to respond to changes in the system which can happen in seconds or milliseconds.

On the other hand, using a very short sample time (i.e. less than one minute) assumes using a special processing platform that computes the optimization process in less than one minute, will force the controller to respond to each change (fluctuations) that the renewable PV generation or load can have. This lead to unsmooth controller actions and may affect the HBSS lifetime since charging and discharging the HBSS, for example every one second, will expose the battery to high stress in operation.

6. The performance of the hierarchical two-layer HEMS

The main drawback of using a single-layer HEMS, observed from the previous experiment, are (a) the single-layer HEMS is greatly affected by the sample time resolution (i.e. using a shorter sample time enables the HEMS to respond faster to the changes in load demand and PV generation, but may conflict with the computation time of the optimization process). On the other hand, using a longer sample time makes the response of the HEMS to changes in the system slower, which affects the overall energy costs and reduction of energy wastage. (b) The single-layer HEMS is greatly affected by the forecasting

uncertainties since the forecasting errors directly lead to inaccurate HBSS power settings and the unwanted imported and/or exported power spikes, that are observed in Fig. 5.b. (c) The single-layer HEMS is affected by the lag of the measurements.

Using a two-layer HEMS will compensate for these drawbacks: (a) the upper layer (MPC layer) will use a longer sample time (i.e. 15 minutes) to avoid computation problems. (b) Instead of directly controlling the HBSS using the MPC layer, which is greatly affected by forecasting errors, sampling time and delay of signals, the MPC layer will determine the stored energy profile for the next 24 hours and pass it to the lower layer (RTC layer). The RTC layer will determine the optimal power settings of the HBSS in real-time, every one minute, using the stored energy profile for the next 24 hours (i.e. obtained from the MPC layer) and a rule-based algorithm. (c) The RTC layer will minimize the energy wastage which results from forecasting errors and sample time, minimize the RES power fluctuations, smooth the fluctuations of the electric power exchanges at the point of common coupling with the grid, through determining the optimal power settings for the HBSS in real-time while taking into account the limits of the required energy stored in the HBSS every sample time period (i.e. obtained from the upper MPC layer).

6.1. Test Procedure

The two-layer HEMS is tested as follows: every sample time (i.e. 15 minutes in this case):

(a) In the upper layer (MPC layer), (1) the forecasted household consumption profile, as well as the forecasted PV generation profile for the next 24 hours, is obtained from the historical data, (2) the values of the actual SOC level of the HBSS are measured from the battery power converter, (3) the MILP optimization process is performed using a MATLAB script, (3) the stored energy profile for the next 24 hours (i.e. the profile uses 15 minute sample time), required for optimal battery operation, is obtained and passed to the RTC layer, (4) the appliance scheduling (i.e. ON/OFF status) obtained for the next 24 hours is sent to each appliance, (5) the previous steps are repeated every 15 minutes.

(b) In the lower layer (RTC layer), The RTC uses the stored energy profile of the HBSS (obtained from MPC layer) in addition to the operating algorithm defined in Fig. 2. to control the battery in real-time every one minute.

6.2. Results

As shown in Fig. 8., the two-layer HEMS managed to control the HBSS in a way to realise the same achievements obtained using the single-layer HEMS in addition to preventing the power spikes that result from forecasting uncertainties, as shown in Fig. 8b. (i.e. compared to results shown in Fig. 5b. using single-layer HEMS). Eliminating power spikes leads to minimize the energy wastage and the overall energy costs. It is also observed that the generated PV energy has been consumed locally in the home instead of being exported to the utility, see Fig. 8.b. From 00:00 to 06:00, during the off-peak tariff period, more

energy has been imported from the utility at a low price (i.e. 4.99 pence/ kWh) to charge the HBSS and cover the household demands. The HBSS is charged from both the imported energy from the utility (during off-peak tariff time) and the surplus PV generation, which is clearly shown in Fig. 8.a. and Fig. 8.d. The daily household energy costs, using the two-layer HEMS, is £0.604 while the energy wastage ratio is 0.18%. The results showed that the daily energy wastage ratio decreased from 26.98%, in case of using single layer HEMS, to 0.18% using the two-layer HEMS – a very significant improvement.

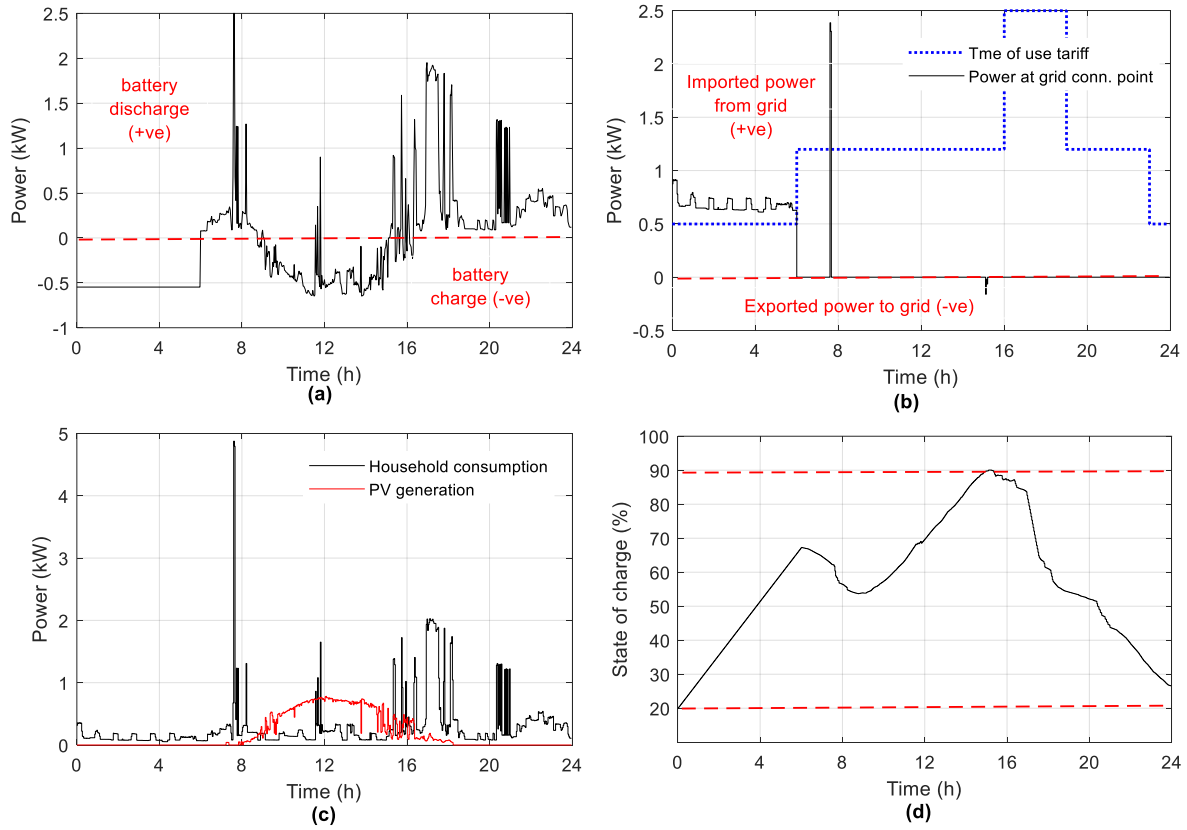

Fig. 8. House rig results using the two-layer HEMS for one day (a) the optimal power settings delivered to the HBSS (a positive value means that the HBSS is discharging, while a negative value means that the HBSS is charging), (b) actual power measured at the grid connection point (a positive value means the house is importing power from the utility, and a negative value means exporting) and the corresponding TOU tariff period, (c) the actual household power demand and PV generation for the current day using a 1 minute sample time, (d) the daily actual state of charge (SOC) of the HBSS.

Table 4 shows the annual simulation results for the case study presented using the two-layer HEMS and the single-layer HEMS. The results show that using the two-layer HEMS achieves lower annual household energy costs compared to using the single-layer HEMS (i.e. a household payment reduction of up to 27.8 % per annum compared to using a single-layer HEMS). The annual PV self-consumption

increased from 78.8% to 91.1 % after using the two-layer HEMS. Also, the two-layer HEMS managed to minimize the annual energy wastage to 8.9%, compared to 21.2% using single-layer HEMS. The reason for not achieving 100% annual PV self-consumption, using the two-layer HEMS, is the selected battery size. The size of the battery is selected to minimize the annual household costs, i.e. investment and operational costs, and hence, using a larger battery size to capture all the surplus PV generation, to achieve 100% PV self-consumption, may increase the annual household costs and reduce the return on investment.

Table 4. Annual household energy costs, annual energy wastage ratio, annual PV self-consumption ratio, and annual forecasting errors using the two-layer HEMS versus using single-layer HEMS.

	Single-layer HEMS	Two-layer HEMS
Annual household energy costs	£ 305.5	£ 220.4
Annual energy wastage ratio	21.2 %	8.9 %
Annual PV self-consumption	78.8 %	91.1 %
Annual forecasting error for the household consumption using L-PWSD forecasting method	34.3 % MAPE	28.27 % MAPE
Annual forecasting error for the PV generation using PV-PD forecasting method	25.4 % MAPE	20.39 % MAPE

The limitations of the proposed hierarchical two-layer HEMS are: (a) it needs additional control devices (loops) to use it in the isolated microgrid systems, i.e. the HBSS should operate in “grid forming” mode when in an isolated microgrid, compared to operating in “grid following” mode in the grid connected mode. (b) If the response time of the battery to the real-time controller’s settings is not fast, the performance may be affected.

7. Conclusion

The hierarchical two-layer home energy management system, presented in this paper, managed to reduce the daily household energy costs, maximize photovoltaic self-consumption and minimize energy wastage compared to using single-layer home energy management system. The management system is tested using a model for a home microgrid system, in which all the constraints that may affect the daily operation are taken into account. The degradation cost model of battery is developed to accurately reflect the explicit battery degradation process and its effect on the daily and annual energy costs. The effectiveness of the proposed home energy management system structure is demonstrated by comparing the obtained results with those from a single-layer system.

The results show that, for the same battery size, using the two-layer home energy management system can achieve a photovoltaic self-consumption of up to 91.1% per annum, compared to using single layer

home energy management system which achieves 78.8% only. The two-layer home energy management system achieves a household payment reduction of up to 27.8% per annum, compared to using single-layer home energy management system. The proposed home energy management system took into account the possibility of load shifting to achieve a greater reduction in household costs by shifting the loads from operating at peak-tariff periods to operate at off-peak tariff periods.

The results obtained show the importance of selecting a shorter sample time and its effect on the performance of the single-layer home energy management system. Using a short sample time (e.g. two minute sample time), for the operation of the single-layer home energy management system, achieves a 29% reduction in the daily household operation costs and a significant reduction in the ratio of RES energy exported to the grid (from 44.68% to 0.5%), compared to using a long sample time of 60 minutes.

The results obtained show that using the two-layer home energy management system to control the home battery storage system through first defining the battery energy stored profile, for the next 24 hour, and then allowing the real-time controller to control the battery in real-time achieved better results compared to directly controlling the battery using the single-layer home energy management system. Using the two-layer home energy management system compensates for uncertainty in energy forecasting as well as the sample time resolution. The two-layer management strategy used a real-time controller to respond to the changes in the load and generation that occur at a short sample time, therefore guarantee better performance and more reduction in costs for the householders.

Using the historical data for household consumption and photovoltaic generation to forecast the next day's load demand and photovoltaic generation profiles minimizes the dependence on external communication technologies (i.e. no need for complex forecasting packages that require additional meteorological data), which makes this control hierarchy a reasonable solution for remote areas which suffer from a poor communication network.

It should be noted that even though the energy management system presented in this paper has been evaluated for a UK domestic residence, the techniques proposed are applicable to households in other countries.

Acknowledgment

This work is supported by the University of Nottingham, the Egyptian Government- ministry of higher education (cultural affairs and missions sector) and the British Council through Newton-Mosharafa fund.

References

[1] Chandra L, Chanana S. Energy Management of Smart Homes with Energy Storage, Rooftop PV and Electric Vehicle. 2018 IEEE International Students' Conference on Electrical, Electronics and Computer Science (SCEECS).

[2] Nizami M, Hossain M, Amin BR, Fernandez E. A residential energy management system with bi-level optimization-based bidding strategy for day-ahead bi-directional electricity trading. Applied Energy. 2020;261:114322.

[3] Xu D, Liu J, Yan X-G, Yan W. A novel adaptive neural network constrained control for a multi-area interconnected power system with hybrid energy storage. IEEE Transactions on Industrial Electronics. 2017;65(8):6625-34.

[4] Wang G, Zhang Q, Li H, McLellan BC, Chen S, Li Y, et al. Study on the promotion impact of demand response on distributed PV penetration by using non-cooperative game theoretical analysis. Applied energy. 2017;185:1869-78.

[5] Ikeda S, Ooka R. Metaheuristic optimization methods for a comprehensive operating schedule of battery, thermal energy storage, and heat source in a building energy system. Applied energy. 2015;151:192-205.

[6] Erdinc O. Economic impacts of small-scale own generating and storage units, and electric vehicles under different demand response strategies for smart households. Applied Energy. 2014;126:142-50.

[7] Erdinc O, Paterakis NG, Mendes TD, Bakirtzis AG, Catalão JP. Smart household operation considering bi-directional EV and ESS utilization by real-time pricing-based DR. IEEE Transactions on Smart Grid. 2014;6(3):1281-91.

[8] Paterakis NG, Taşcıkaraoğlu A, Erdinc O, Bakirtzis AG, Catalao JP. Assessment of demand-response-driven load pattern elasticity using a combined approach for smart households. IEEE Transactions on Industrial Informatics. 2016;12(4):1529-39.

[9] Tsui KM, Chan S-C. Demand response optimization for smart home scheduling under real-time pricing. IEEE Transactions on Smart Grid. 2012;3(4):1812-21.

[10] Melhem FY, Grunder O, Hammoudan Z, Moubayed N. Optimization and energy management in smart home considering photovoltaic, wind, and battery storage system with integration of electric vehicles. Canadian Journal of Electrical and Computer Engineering. 2017;40(2):128-38.

[11] Zhang Y, Wang R, Zhang T, Liu Y, Guo B. Model predictive control-based operation management for a residential microgrid with considering forecast uncertainties and demand response strategies. IET Generation, Transmission & Distribution. 2016;10(10):2367-78.

[12] Terlouw T, AlSkaif T, Bauer C, van Sark W. Multi-objective optimization of energy arbitrage in community energy storage systems using different battery technologies. Applied Energy. 2019;239:356-72.

[13] Ahmed MS, Mohamed A, Khatib T, Shareef H, Homod RZ, Ali JA. Real time optimal schedule controller for home energy management system using new binary backtracking search algorithm. Energy and Buildings. 2017;138:215-27.

[14] Zhang Y, Campana PE, Lundblad A, Yan J. Comparative study of hydrogen storage and battery storage in grid connected photovoltaic system: Storage sizing and rule-based operation. Applied energy. 2017;201:397-411.

[15] Purvins A, Sumner M. Optimal management of stationary lithium-ion battery system in electricity distribution grids. Journal of Power Sources. 2013;242:742-55.

[16] Teleke S, Baran ME, Bhattacharya S, Huang AQ. Rule-based control of battery energy storage for dispatching intermittent renewable sources. IEEE Transactions on Sustainable Energy. 2010;1(3):117-24.

[17] Jin X, Wu J, Mu Y, Wang M, Xu X, Jia H. Hierarchical microgrid energy management in an office building. Applied energy. 2017;208:480-94.

[18] Ke X, Lu N, Jin C. Control and size energy storage systems for managing energy imbalance of variable generation resources. IEEE Transactions on Sustainable Energy. 2014;6(1):70-8.

[19] Parisio A, Rikos E, Glielmo L. A model predictive control approach to microgrid operation optimization. IEEE Transactions on Control Systems Technology. 2014;22(5):1813-27.

[20] Terlouw T, AlSkaif T, Bauer C, van Sark W. Optimal energy management in all-electric residential energy systems with heat and electricity storage. Applied Energy. 2019;254:113580.

[21]nagement system for energy efficiency and demand response. Applied Energy. 2017;205:1583-95.

[22] Di Piazza M, La Tona G, Luna M, Di Piazza A. A two-stage Energy Management System for smart buildings reducing the impact of demand uncertainty. Energy and Buildings. 2017;139:1-9.

[23] Elkazaz M, Sumner M, Thomas D. Energy management system for hybrid PV-wind-battery microgrid using convex programming, model predictive and rolling horizon predictive control with experimental validation. International Journal of Electrical Power & Energy Systems. 2020;115:105483.

[24] Palma-Behnke R, Benavides C, Lanas F, Severino B, Reyes L, Llanos J, et al. A microgrid energy management system based on the rolling horizon strategy. IEEE Transactions on smart grid. 2013;4(2):996-1006.

[25] Zhang Y, Zhang T, Wang R, Liu Y, Guo B. Optimal operation of a smart residential microgrid based on model predictive control by considering uncertainties and storage impacts. Solar Energy. 2015;122:1052-65.

[26] Luo F, Ranzi G, Kong W, Dong ZY, Wang F. Coordinated residential energy resource scheduling with vehicle-to-home and high photovoltaic penetrations. IET Renewable Power Generation. 2018;12(6):625-32.

[27] Iwafune Y, Ikegami T, da Silva Fonseca Jr JG, Oozeki T, Ogimoto K. Cooperative home energy management using batteries for a photovoltaic system considering the diversity of households. Energy Conversion and Management. 2015;96:322-9.

[28] Elkazaz M, Sumner M, Pholboon S, Thomas D. Microgrid Energy Management Using a Two Stage Rolling Horizon Technique for Controlling an Energy Storage System. 2018; IEEE 7th International Conference on Renewable Energy Research and Applications (ICRERA).

[29] Terlouw T, Zhang X, Bauer C, Alskaif T. Towards the determination of metal criticality in home-based battery systems using a Life Cycle Assessment approach. Journal of Cleaner Production. 221 (2019): 667-677.

[30] I.S. ASSOCIATION. IEEE Guide for the Characterization and Evaluation of Lithium-Based Batteries in Stationary Applications. 2017.

[31] Hoke A, Brissette A, Maksimović D, Pratt A, Smith K. Electric vehicle charge optimization including effects of lithium-ion battery degradation. 2011; IEEE Vehicle Power and Propulsion Conference.

[32] Sun Y, Yue H, Zhang J, Booth C. Minimization of residential energy cost considering energy storage system and EV with driving usage probabilities. IEEE Transactions on Sustainable Energy. 2018;10(4):1752-63.

[33] Chalise S, Sternhagen J, Hansen TM, Tonkoski R. Energy management of remote microgrids considering battery lifetime. The Electricity Journal. 2016;29(6):1-10.

[34] Garcia-Torres F, Bordons C. Optimal economical schedule of hydrogen-based microgrids with hybrid storage using model predictive control. IEEE Transactions on Industrial Electronics. 2015;62(8):5195-207.

[35] Richardson I, Thomson M. Domestic electricity use: a high-resolution energy demand model. Energy and Buildings, 2010; 42 (10):1878-1887

[36] UK power. Average gas and electric usage for UK households, https://www.ukpower.co.uk/home_energy/average-household-gas-and-electricity-usage [accessed March 2020].

[37] PVOutput. Generation profiles for a 3.8 kW PV station located in Nottingham, https://pvoutput.org/ [accessed March 2020].

[38] Money Saving Expert. time-of-day purchasing tariff in UK, https://www.moneysavingexpert.com/news/2017/01/green-energy-launches-time-of-day-tariff---electricity-savings-available-but-gas-remains-pricey/ [accessed March 2020].

[39] Ofgem. Feed-In Tariff (FIT) rates in UK, https://www.ofgem.gov.uk/environmental-programmes/fit/fit-tariff-rates;2020 [accessed March 2020].

[40] Wikipedia. Electricity price comparison across countries, https://en.wikipedia.org/wiki/Electricity_pricing [accessed March 2020].

[41] Bahramirad S, Reder W, Khodaei A. Reliability-constrained optimal sizing of energy storage system in a microgrid. IEEE Transactions on Smart Grid. 2012;3(4):2056-62.

[42] BloombergNEF. A Behind the Scenes Take on Lithium-ion Battery Prices, https://about.bnef.com/blog/behind-scenes-take-lithium-ion-battery-prices/; 2019 [accessed March 2020].

[43] ALMASOALR. SMA power inverters prices list, https://www.alma-solarshop.com/131-sma-inverter#/;2019 [accessed March 2020].

[44] CCL. BYD B-BOX HV - LITHIUM BATTERY PACK, https://www.cclcomponents.com/byd-b-box-high-voltage-6-4kwh-lithium-battery [accessed March 2020]].

[45] SMA. SUNNY BOY STORAGE 2.5 power inverter, https://www.anh-technologies.co.za/pdf/sma_sunny_boy_15-25.pdf [accessed March 2020].

[46] Antonanzas J, Osorio N, Escobar R, Urraca R, Martinez-de-Pison F, Antonanzas-Torres F. Review of photovoltaic power forecasting. Solar Energy. 2016;136:78-111.

[47] FF-GRID EUROPE. SMA INTEGRATED STORAGE SYSTEM SB 3600 SMART ENERGY INVERTER, https://www.off-grid-europe.com/sma-integrated-storage-system-sb-3600-smart-energy-inverter?gclid=CjwKCAjw5fzrBRASEiwAD2OSV8QTkNn5Es4NLxChBekDTGV1-Qt1HfModDjrFphFK49LY05ftgj1cRoCWhkQAvD_BwE [accessed March 2020].

[48] CALTEST Instrumnts Ltd. ZSAC Series – AC Loads – Hoecherl & hackl, https://www.caltest.co.uk/product/zsac-series/ [accessed March 2020].

[49] NATIONAL INSTRUMENTS. CompactRIO Systems, https://www.ni.com/en-gb/shop/compactrio.html [accessed March 2020].

[50] Smart process& control Ltd. SMARTRAIL X835-MID DIN Rail Multifunction Power Meter, http://www.smartprocess.co.uk/PDF/Smart-Process_SMARTRAIL-X835-MID_Datasheet.pdf [accessed March 2020].